Journal of Power Sources 196 (2011) 6637–6643

Contents lists available at ScienceDirect

Journal of Power Sources

journal homepage: www.elsevier.com/locate/jpowsour

Si thin platelets as high-capacity negative electrode for Li-ion batteries

Morihiro Saito[a], Kenta Nakai[a], Tomoyuki Yamada[a], Toshio Takenaka[b], Makoto Hirota[b], Akika Kamei[b], Akimasa Tasaka[a], Minoru Inaba[a,*]

[a] Department of Molecular Chemistry and Biochemistry, Faculty of Science, Doshisha University, Kyotanabe, Kyoto 610-0321, Japan
[b] Oike & Co., Ltd., Kamitoba, Minami-ku, Kyoto 610-8121, Japan

ARTICLE INFO

Article history:
Received 22 September 2010
Received in revised form 17 February 2011
Accepted 17 February 2011
Available online 24 February 2011

Keywords:
Li–Si alloy negative electrode
Thin platelets
High capacity
Cycleability
Irreversible capacity

ABSTRACT

Pure Si platelets and Ni or Cu layer-laminated Si platelets with difference thickness were prepared, and their charge/discharge properties were examined in 1 M $LiClO_4$/EC + DEC (1:1 by volume) as alternative negative electrode materials to graphite for Li-ion batteries. The shape of thin platelets and lamination with Ni layer are significantly effective to improve the cycleability in Li–Si alloy system by relieving the stress during the alloying/de-alloying processes, reinforcing the mechanical strength and reducing the Li^+ ion diffusion length. Moreover, the first irreversible capacity is minimized by reduction of the amount of Ketjen Black (KB) in the composite electrode because of electrolyte decomposition on the surface of KB. Consequently, the Si/Ni/Si-LP30 (30/30/30 nm) composite electrode with 5 wt% KB also exhibits over 700 mAh g^{-1} even after 50 cycles in 1 M $LiPF_6$/EC + DEC (1:1).

1. Introduction

Li–Si alloy systems have attracted much attention as negative electrodes in lithium-ion cells because of their high theoretical capacity (ca. 4200 mAh g^{-1}) [1,2]. However, the capacity retention of Si is poor, and it shows a high irreversible capacity in the first charge/discharge cycle. The poor retention is ascribed to a large volume expansion and contraction during the charge/discharge cycling, which causes particle fracture and electrochemical pulverization [3]. As a result, a significant capacity loss upon cycling is induced. Therefore, relaxation of the stress caused by the expansion and contraction of Li–Si alloy materials is important to obtain a good cycleability. This concept has been realized by using Si nanoparticles [3–10] or nanowires [11–16], which are usually used as composites with carbon or SiO_x (Si/C or Si/SiO_x) [3–12]. Another concept is to use thin films of metals [17–21]; however, the thickness of the film should be less than several micrometers to obtain good cycleability, which limits the capacity of the cells. From these viewpoints, metal thin platelets are a promising morphology for alloy materials to attain both high capacity and good cycleability [22,23]. In addition, lamination with inactive metals such as Ni can increase the strength of the platelets, by which further improved cycleability is expected, though the specific capacity decreases.

In this study, we prepared five types of Si thin platelets (Leaf Powder®, Oike & Co., Ltd.) as shown in Fig. 1, and examined the charge/discharge characteristics. The morphologies of the samples before and after the charge/discharge cycling and components of solid electrolyte interphase (SEI) are also investigated.

2. Experimental

Pure Si platelets (Si-LP, thickness: 100 nm) and Ni or Cu layer-laminated Si platelets with difference thickness (Si/Ni/Si-LP30 (30/30/30 nm), Si/Ni/Si-LP50 (50/50/50 nm), Ni/Si/Ni-LP (15/60/15 nm) and Si/Cu/Si-LP30 (30/30/30 nm)) were prepared by a physical vapor deposition (PVD) method using vacuum evaporation, followed by crashing. The size of the platelets was controlled in 4–5 μm square with a thickness of 90–150 nm. Commercially available Si powder (Aldrich, <325 mesh) was also used for comparison. The test electrode was fabricated by coating slurry on a copper foil as a current collector. The slurry was prepared by mixing (90 − *x*) wt% active material sample, *x* wt% Ketjen Black (KB, Lion Corp., EC600JD) as a conductive agent and 10 wt% carboxymethyl cellulose sodium (NaCMC) salt as a binder using water as a solvent. The slurry was coated on a copper foil current collector (0.785 cm^2) with a thickness of 50 μm, and then dried overnight at 80 °C under vacuum. The electrochemical evaluation was performed by constant current–constant voltage (CC–CV) charge/discharge tests with a coin-type two-electrode half-cell. The counter electrode was Li foil. The electrolyte solution was 1 M $LiClO_4$ or 1 M $LiPF_6$ dissolved in EC/DEC (1:1, by volume). The surface morphologies of

* Corresponding author. Tel.: +81 774 65 6591; fax: +81 774 65 6841.
E-mail address: minaba@mail.doshisha.ac.jp (M. Inaba).

0378-7753/$ – see front matter © 2011 Elsevier B.V. All rights reserved.
doi:10.1016/j.jpowsour.2011.02.042

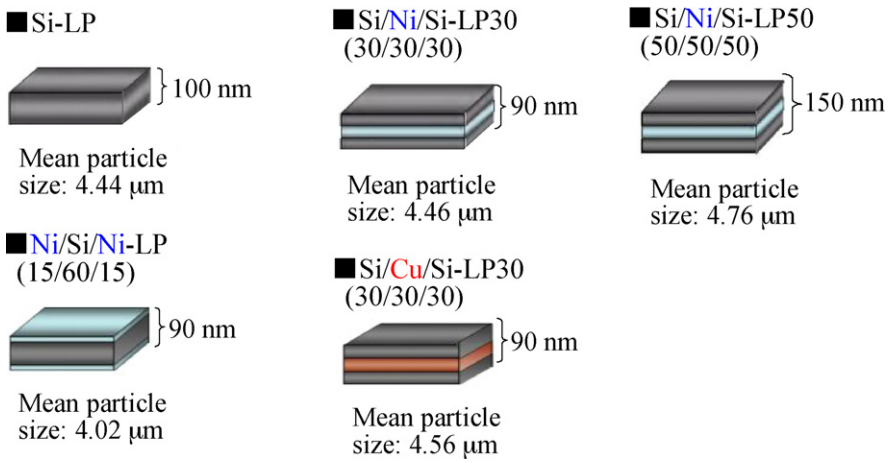

Fig. 1. Schematic illustrations of the Si thin platelets.

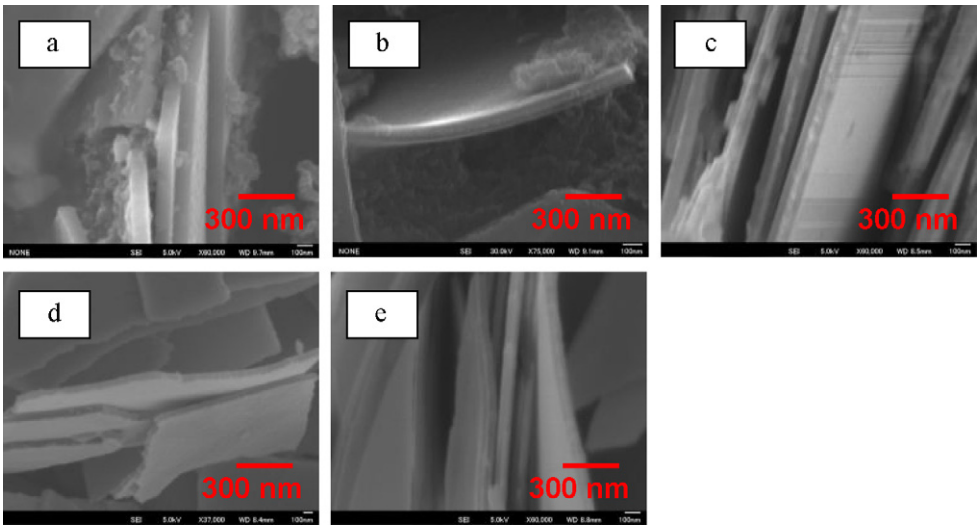

Fig. 2. SEM images for Si thin platelets. (a) Si-LP, (b) Si/Ni/Si-LP30, (c) Si/Ni/Si-LP50, (d) Ni/Si/Ni-LP and (e) Si/Cu/Si-LP30.

the electrodes before and after CC–CV tests and components of SEI were examined by a scanning electron microscope (SEM) with a secondary electron detector and X-ray photoelectron spectroscopy (XPS), respectively.

3. Results and discussion

3.1. Characterizations of Si thin platelets

Fig. 2 shows the SEM images of the Si thin platelets. They had platelet structure with an average size of 4–5 μm. The thicknesses of the Si-LP, Si/Ni/Si-LP30, Si/Ni/Si-LP50, Ni/Si/Ni-LP and Si/Cu/Si-LP30 were 100, 90, 150, 90 and 90 nm, respectively. The presence of the Ni and Cu layers was confirmed in the laminated samples, especially clearly in the Si/Ni/Si-LP50.

XRD patterns of the platelets are shown in Fig. 3. For commercially available Si powder, sharp peaks assigned to Si(1 1 1), Si(2 2 0) and Si(3 1 1) were clearly observed. In contrast, no clear peaks assigned to crystalline Si were observed for all the platelets, which indicated that Si in the thin platelets was amorphous. On the pattern of the Si-LP, a small peak was found at around 38°, which is probably assigned to SiO_2. This indicates that a relatively large amount of SiO_2 covered the surface of Si-LP as compared with those of the other laminated platelets.

3.2. Electrochemical properties and cycleability of Si thin platelets

Fig. 4 shows the charge/discharge curves of Si thin platelets and Si powder. The Si powder and Si-LP showed high initial discharge capacities of over 2000 mAh g^{-1}, while the other laminated

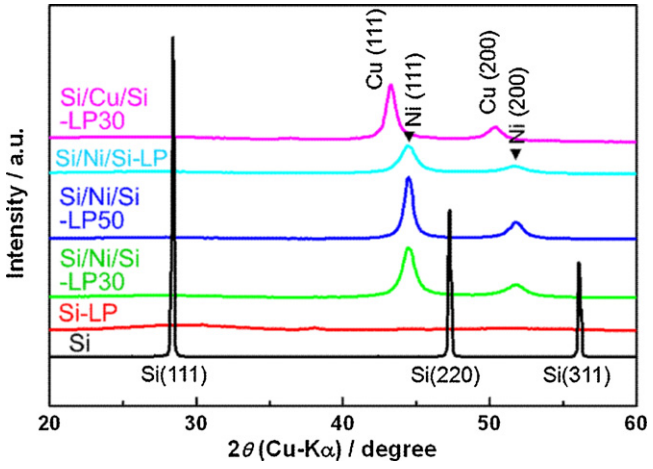

Fig. 3. XRD patterns of Si thin platelets together with a conventional Si powder.

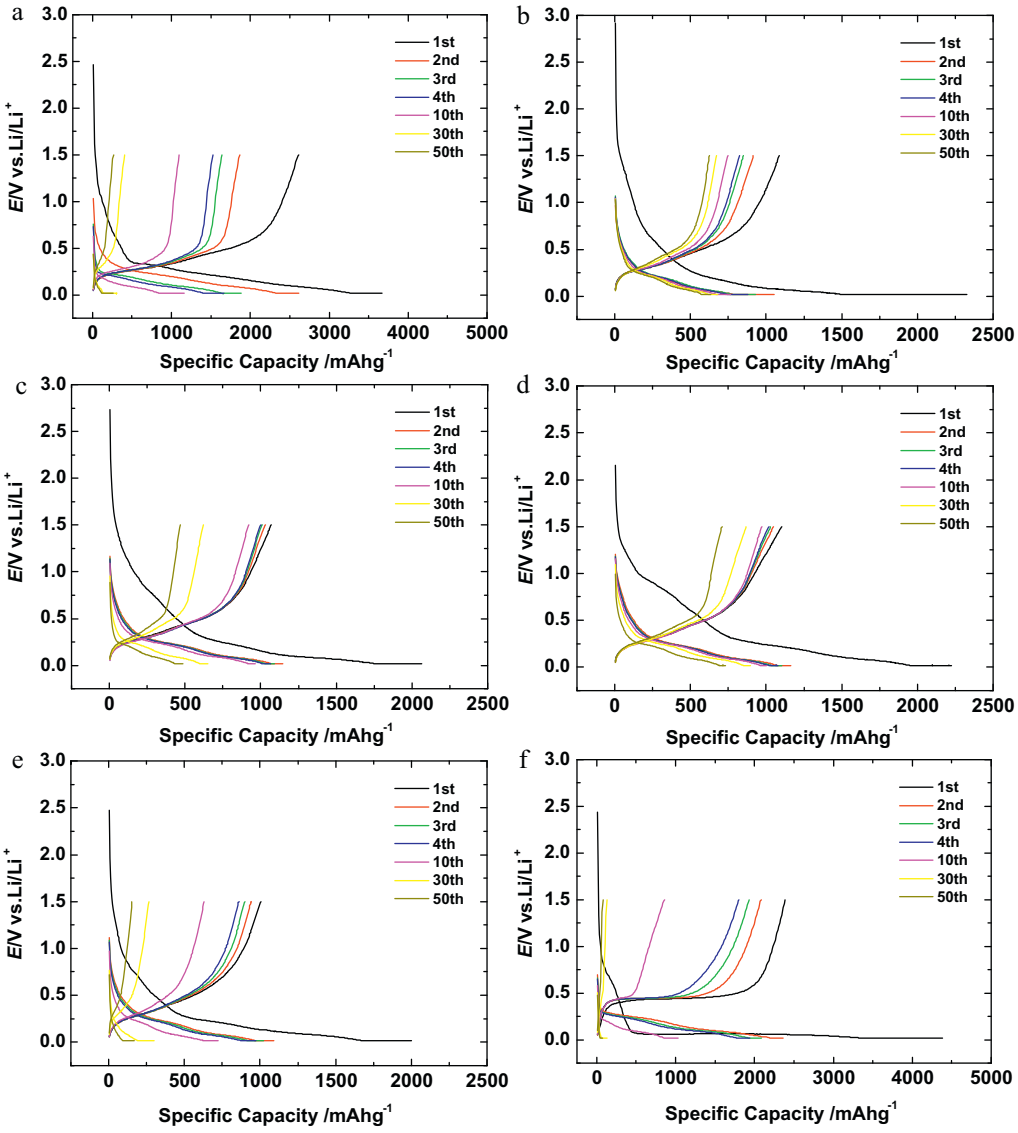

Fig. 4. Charge/discharge curves of (a) Si-LP, (b) Si/Ni/Si-LP30, (c) Si/Ni/Si-LP50, (d) Ni/Si/Ni-LP, (e) Si/Cu/Si-LP30 and (f) Si powder electrodes consisted of active material + KB + NaCMC = 75:15:10 by weight at C/6 in 1 M $LiClO_4$/EC + DEC (1:1 by volume). Potential range: 0.02–1.5 V vs. Li/Li^+.

Si platelets exhibited lower initial capacities of ca. 1000 mAh g^{-1} because of the presence of inactive Ni or Cu layer. The charge current was observed at around 1.5–0.75 V in the first charging for all the platelets. However, in the second charging, it began to appear below 0.5 V. In addition, all the platelets showed large irreversible capacities in the first cycle. These results indicate that solid electrolyte interphase (SEI) was formed on the surface of electrode through the reductive decomposition of electrolyte. For the

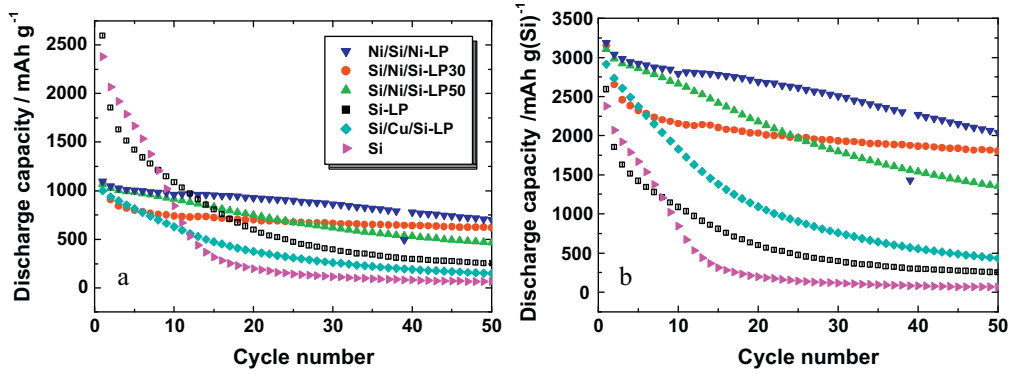

Fig. 5. (a) Discharge capacity and (b) coulombic efficiency vs. cycle number of Si/Ni/Si-LP30, Si/Ni/Si-LP50, Ni/Si/Ni-LP and Si/Cu/Si-LP30 electrodes consisted of active material + KB + NaCMC = 75:15:10 by weight at C/6 in 1 M $LiClO_4$/EC + DEC (1:1 by volume). Potential range: 0.02–1.5 V vs. Li/Li^+.

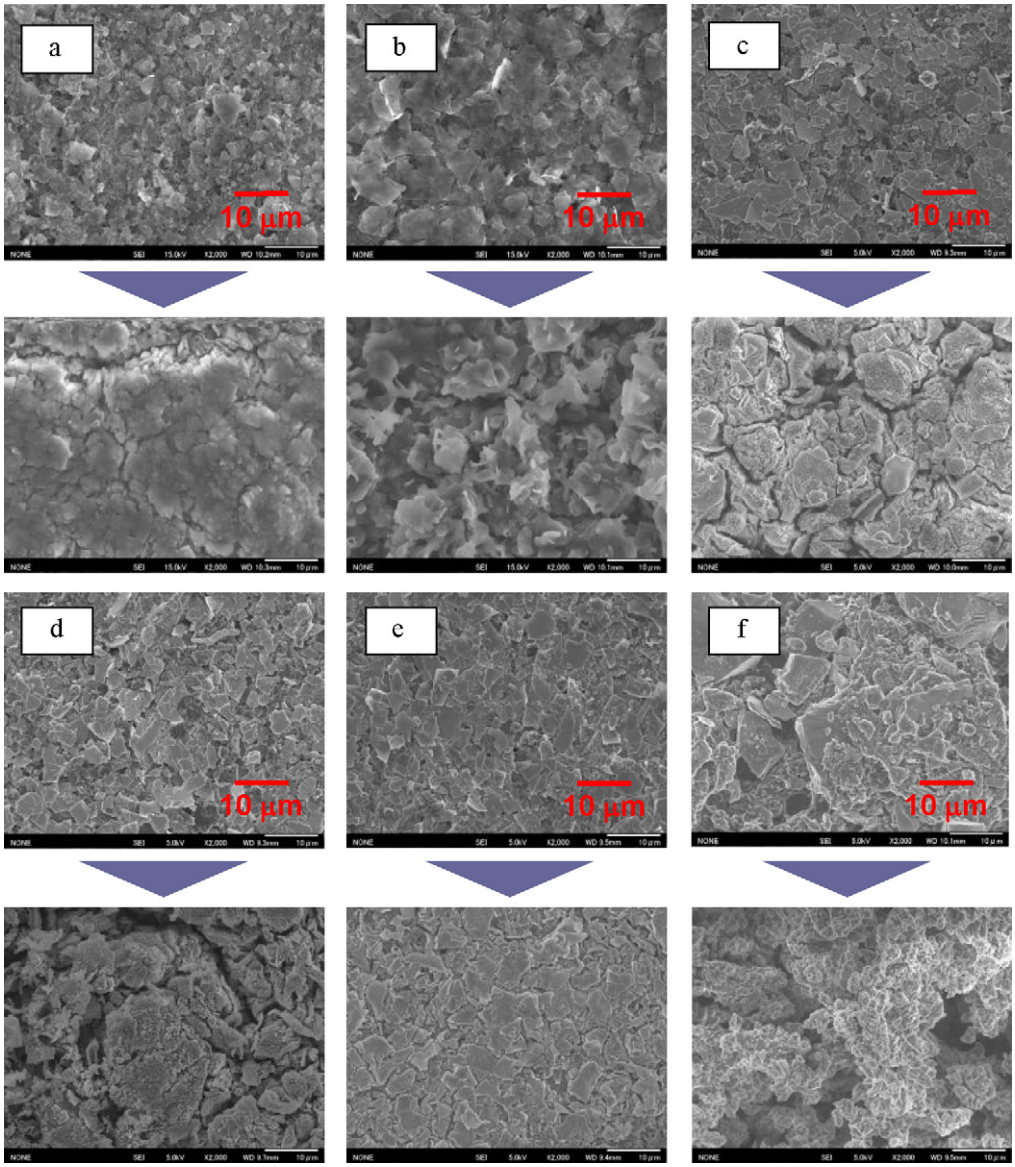

Fig. 6. SEM images of Si thin platelets after the CC–CV tests. (a) Si-LP, (b) Si/Ni/Si-LP30, (c) Si/Ni/Si-LP50, (d) Ni/Si/Ni-LP, (e) Si/Cu/Si-LP30 and (f) Si powder.

Si powder, the discharge current began to appear at around 0.5 V; however, it was at around 0.25 V for the Si thin platelets. Therefore, hysteresis between the charge and discharge curves was found to be smaller for the Si thin platelets, probably because Si in the platelets was amorphous.

Cycleability of the Si thin platelets and Si powder are shown in Fig. 5(a). In the case of the Si powder, the charge and discharge capacity dropped drastically in several cycles and it became hard to charge and discharge after only 15 cycles. The Si-LP showed improved cycleability. Though the initial discharge capacity was lower than that of the Si and Si-LP, the laminated Si platelets showed excellent retention of the charge/discharge capacity. The Si/Ni/Si-LP30 showed the best retention of the charge/discharge capacity among the laminated platelets. Therefore, both concepts of shape control and lamination are found to be effective to improve the cycleability in Li–Si alloy system. However, the cycleability of Si/Cu/Si-LP30 was poor as compared with other Leaf Powders that were laminated with Ni layer.

To elucidate the utilization of Si in the laminated Si thin platelets, the practical discharge capacity was converted against the Si mass (Fig. 5(b)). The Si utilization in the first cycle was ca. 3200 mAh g^{-1} for the laminated Si thin platelets, i.e. more than 75% of theoretical capacity (ca. 4200 mAh g^{-1}) of Si, while the Si powder and Si-LP was ca. 60% of the theoretical value. This implies that the alloying and de-alloying reactions proceed more effectively and reversibly in the laminated platelets, which is probably attributed to enhancement of the mechanical strength against crack formation and pulverization, and further reduction of the diffusion length of Li^+ ions.

Fig. 6 shows the SEM images of Si platelets and Si powder before and after 50 cycles. The initial large particles of the commercially available Si powder were pulverized after repeated charging and discharging. On the other hand, agglomeration of thin flakes was observed for Si-LP. In contrast to Si-LP, for Si/Ni/Si-LP30, Si/Ni/Si-LP50, Ni/Si/Ni-LP and Si/Cu/Si-LP30, thin flakes of platelet remained after 50 cycles, while some agglomeration was observed in Si/Ni/Si-LP50 and Ni/Si/Ni-LP. Therefore the presence of the inert metal layer suppressed the agglomeration of thin flakes. In summary, laminated platelets effectively prevented pulverization and remained their shape by containing inert metal layer, which resulted in excellent cycleability. The morphology of Si/Cu/Si-LP hardly changed after 50 cycles. However, the cycleability was poorer than Ni layer laminated LP as shown in Fig. 5(a), the reason of which is not clear

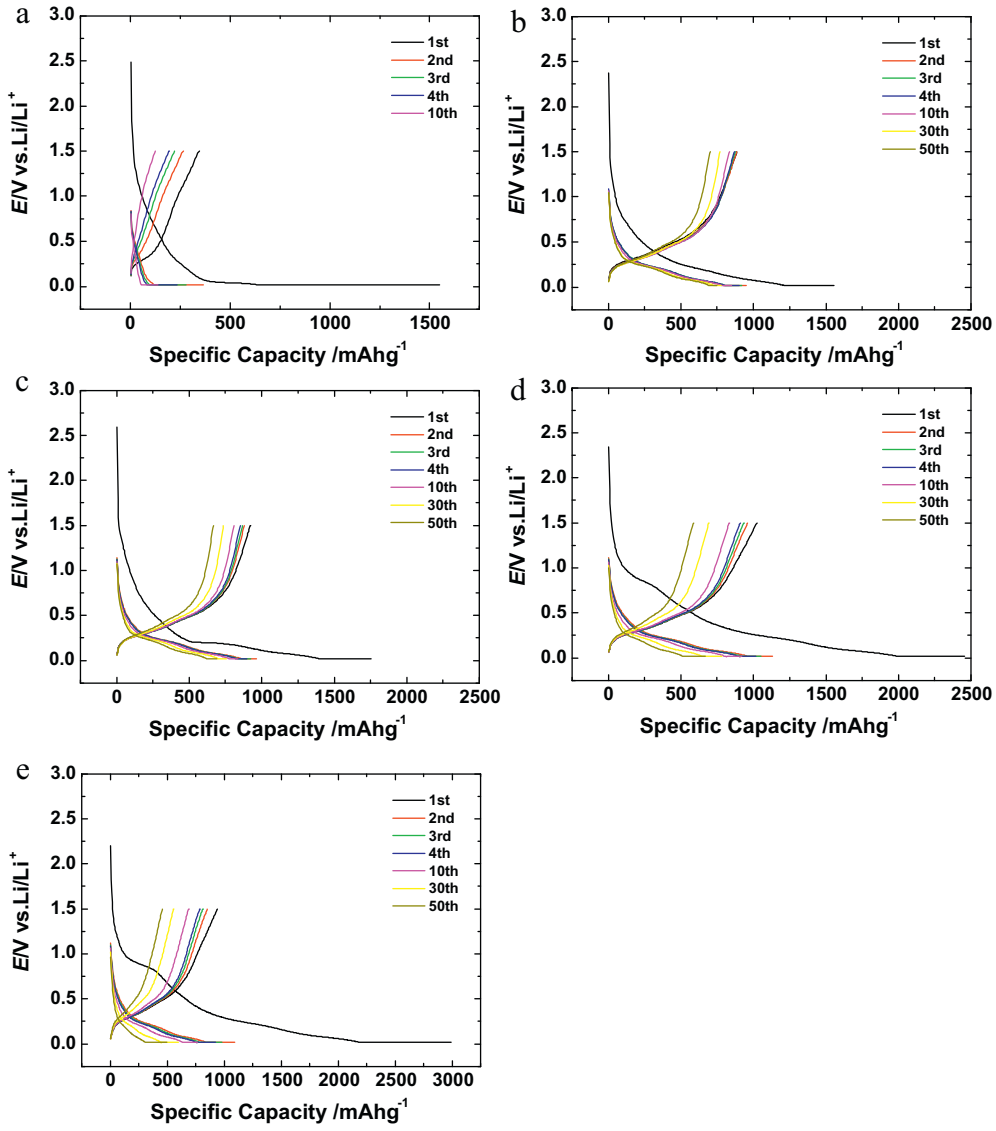

Fig. 7. Charge/discharge curves of Si/Ni/Si-LP30 electrodes consisted of Si/Ni/Si-LP30:KB:NaCMC = (a) 75:0:10, (b) 75:5:10, (c) 75:10:10, (d) 75:20:10, (e) 75:35:10 by weight at C/6 in 1 M $LiClO_4$/EC + DEC (1:1 by volume). Potential range: 0.02–1.5 V vs. Li/Li^+.

at present.

3.3. Decrease in the irreversible capacity at 1st cycle

It is widely known that the KB is superior as an electron-conductive material to the other conductive agents such as the conventional acetylene black (AB). However, the large specific surface area also brings about a greatly large amount of decomposition of electrolyte on the KB, and generates a significant irreversible capacity. Therefore, to reduce the irreversible capacity of the composite electrode, the amount of KB added in the electrode was changed, and their charge/discharge properties were evaluated using the Ni/Si/Ni-LP30 that exhibited the highest cycleability in the above results. Fig. 7 shows the charge/discharge curves of the Ni/Si/Ni-LP30 electrodes containing various amounts of KB. By increasing the amount of KB, a plateau appeared at around 1.0 V on charging, which corresponds to the current due to the decomposition of electrolyte on KB.

The charge and discharge capacities are summarized in Fig. 8. As shown in Fig. 8, the first discharge capacity did not increase at more than 5 wt% of KB, while the first charge capacity increased

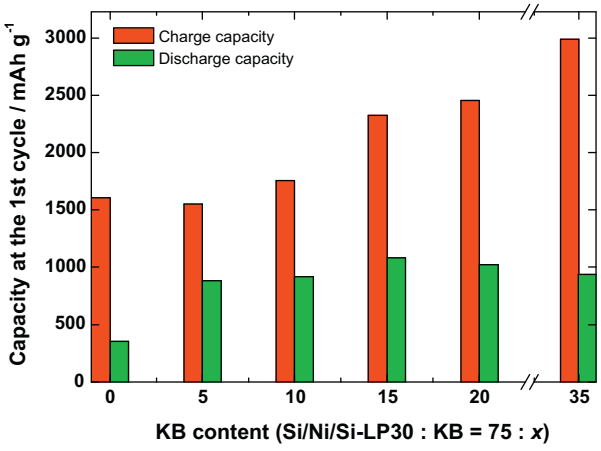

Fig. 8. First charge and discharge capacity of Si/Ni/Si-LP30 electrodes consisted of Si/Ni/Si-LP30 + KB + NaCMC = 75:0:10, 75:5:10, 75:10:10, 75:15:10, 75:20:10, 75:35:10 by weight at C/6 in 1 M $LiClO_4$/EC + DEC (1:1 by volume). Potential range: 0.02–1.5 V vs. Li/Li^+.

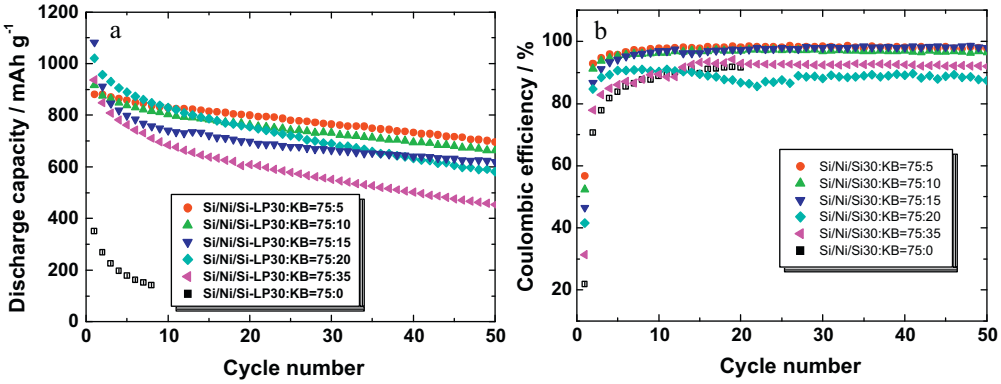

Fig. 9. (a) Discharge capacity and (b) coulombic efficiency vs. cycle number of Si/Ni/Si-LP30 electrodes consisted of Si/Ni/Si-LP30 + KB + NaCMC = 75:0:10, 75:5:10, 75:10:10, 75:15:10, 75:20:10, 75:35:10 by weight at C/6 in 1 M $LiClO_4$/EC + DEC (1:1 by volume). Potential range: 0.02–1.5 V vs. Li/Li^+.

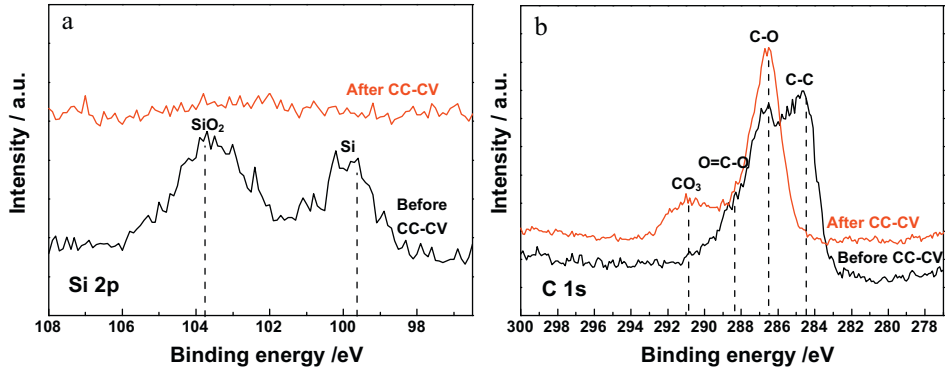

Fig. 10. XPS spectra of (a) Si 2p and (b) C 1s levels on Si/Ni/Si-LP30 electrodes consisted of Si/Ni/Si-LP30 + KB + NaCMC = 75:5:10 by weight before and after 10 cycle at C/6 in 1 M $LiClO_4$/EC + DEC (1:1 by volume). Potential range: 0.02–1.5 V vs. Li/Li^+. Beam current: 10 mA at 15 kV.

with an increase in the amount of KB. This indicates that 5 wt% of KB is enough to make the electron path in the composite electrode, and extra amount of KB provides the irreversible capacity due to the electrolyte decomposition on the surface of KB. As a result, the irreversible capacity was reduced down to of 672 mAh g^{-1} at the 5 wt% of KB, which corresponds to ca. 54% of the irreversible capacity in the case of 15 wt% KB. Therefore, to fabricate the composite electrode using Li–Si alloy anode, it is considered that the kinds and adding amount of conductive agent is important for the practical use. Further optimization of the conductive agents was now in progress.

Fig. 9(a) and (b) shows the discharge capacity and the coulombic efficiency vs. cycle number for the composite electrodes using the Si/Ni/Si-LP30. The composite electrode consisted of Si/Ni/Si-LP30:KB:NaCMC = 75:5:10 exhibited a high capacity of 696 mAh g^{-1} in 50 cycles and the highest cycleability among them (Fig. 9(a)). Also, the coulombic efficiency vs. cycle number at the 5 wt% KB was the highest from the initial cycles (Fig. 9(b)). Non-adding and extra-adding KB over 20 wt% led to decrease the coulombic efficiency.

Fig. 10 shows the XPS spectra for the composite electrode using Si/Ni/Si-LP30 with 5 wt% KB before and after the charge/discharge test. In the Si 2p, the XPS peaks assigned to Si and SiO_2 were clearly observed at 99.6 eV and 103.7 eV, respectively. However, the XPS peaks vanished only after 10 cycles. On the other hand, for the C 1s the XPS spectra of C–C, C–O and O═C–O bonds were confirmed at 184.5 eV, 186.5 eV and 288.4 eV, respectively. However, the XPS spectra completely changed and a new XPS spectra appeared at

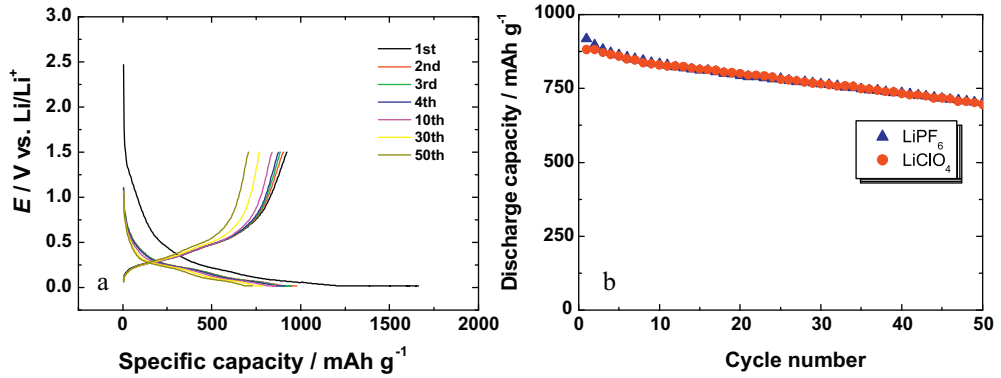

Fig. 11. (a) Charge/discharge curves and (b) cycleability of Si/Ni/Si-LP30 electrode consisted of Si/Ni/Si-LP30 + KB + NaCMC = 75:5:10 by weight at C/6 in 1 M $LiPF_6$/EC + DEC (1:1 by volume). Potential range: 0.02–1.5 V vs. Li/Li^+.

186.5 eV and 290 eV, which are considered to be originated from Li_2CO_3 containing in the SEI. These results indicate that the electrolyte decomposed both on the surface of Si thin platelet and KB to form the SEI film, which causes the large irreversible capacity. In addition, the SiO_2 was also detected on the surface of Si/Ni/Si-LP30. It is well known that the electrochemical reduction of SiO_2 to metal Si generates Li_2O and Li_4SiO_4 as electrochemically inactive by-products [24], which is also an origin of the irreversible capacity at the first charging process. Therefore, the irreversible capacity is suggested to be reduced by decreasing the amount of SiO_2.

For the practical use of the Si thin platelets, availability of a conventional Li salt $LiPF_6$ is quite important because of the physical properties. Fig. 11(a) and (b) shows the charge/discharge curves and cycleability for the Si/Ni/Si-LP30. From the results, the charge/discharge performance was not changed in 1 M $LiPF_6$/EC + DEC (1:1 by volume) at C/6 rate. The estimated coulombic efficiency vs. cycle number was also excellent.

4. Conclusions

To improve the capacity retention of Li–Si alloy anode, five kinds of Si thin platelets were prepared, and their charge/discharge properties were examined. The shape of thin platelets effectively relieved the stress by volume expansion and shrinkage during the alloying and de-alloying processes with Li^+ ion, and greatly improved the cycleability. The lamination with the Li-inactive Ni layer further improved the cycleability by reinforcing the platelets and reducing the diffusion length of Li^+ ions, though the specific capacity decreased by its presence. As the results, the Si/NiSi-LP30 showed the best cycle performance. On the other hand, a part of irreversible capacity at the 1st cycle was found to be originated from the electrolyte decomposition on KB by charge/discharge test using various amounts of KB and XPS analysis. The irreversible capacity was minimized to 672 mAh g^{-1} by reduction of the amount of KB in the composite electrode down to 5 wt%. Moreover, for the practical use of Si thin platelets, the charge/discharge properties of Si/Ni/Si-LP30 was evaluated in the $LiPF_6$-based electrolyte, and was demonstrated to exhibit an excellent performance as well as that in the $LiClO_4$-based one. Consequently, a high first discharge capacity of 917 mAh g^{-1} was obtained, and more than 700 mAh g^{-1} was kept in 50 cycles.

Acknowledgment

This work was supported by “Kyoto Environmental Nanotechnology Cluster” from MEXT, Japan.

References

[1] R.A. Huggins, J. Power Sources 81–82 (1999) 13.
[2] B.A. Boukamp, G.C. Lesh, R.A. Huggins, J. Electrochem. Soc. 128 (1981) 725.
[3] H. Li, X. Huang, L. Chen, Z. Wu, Y. Liang, Electrochem. Solid-State Lett. 2 (1999) 547.
[4] J. Yang, B.F. Wang, K. Wang, Y. Liu, J.Y. Xie, Z.S. Wen, Solid-State Lett. 6 (2003) A154.
[5] U. Kasavajjula, C. Wang, A.J. Appleby, J. Power Sources 163 (2007) 1003.
[6] H. Kim, M. Seo, M.-H. Park, J. Cho, Angew. Chem. Int. Ed. 49 (2010) 2146.
[7] J. Yang, Y. Takeda, N. Imanishi, C. Capiglia, J.Y. Xie, O. Yamamoto, Solid State Ionics 152–153 (2002) 125.
[8] T. Morita, N. Takami, J. Electrochem. Soc. 153 (2006) A425.
[9] Y.-S. Hu, R. Demir-Cakan, M.-M. Tittrici, J.-O. Müller, R. Schlögl, M. Antonietti, J. Maier, Angew. Chem. Int. Ed. 47 (2008) 1645.
[10] C.-M. Park, W. Choi, Y. Hwa, J.-H. Kim, G. Jeong, H.-J. Sohn, J. Mater. Chem. 20 (2010) 4854.
[11] H. Kim, J. Cho, Nano Lett. 8 (2008) 3688.
[12] L.-F. Cui, Y. Yang, C.-M. Hsu, Y. Cui, Nano Lett. 9 (2009) 3370.
[13] C.K. Chan, H. Peng, G. Liu, K. McIlwrath, X.F. Zhang, R.A. Huggins, Y. Cui, Nat. Nanotechnol. 3 (2008) 31.
[14] L.-F. Cui, R. Ruffo, C.K. Chan, H. Peng, Y. Cui, Nano Lett. 9 (2009) 491.
[15] C.K. Chan, R. Ruffo, S.S. Hong, R.A. Huggins, Y. Cui, J. Power Sources 189 (2009) 34.
[16] X. Chen, K. Gerasopoulos, J. Guo, A. Brown, C. Wang, R. Ghodssi, J.N. Culver, ACS Nano 4 (2010) 5366.
[17] T. Takamura, S. Ohara, M. Uehara, J. Suzuki, K. Sekine, J. Power Sources 129 (2004) 96.
[18] H. Guo, H. Zhao, C. Yin, W. Qiu, Mater. Sci. Eng. B 131 (2006) 173.
[19] T.L. Kulova, A.M. Skundin, Yu.V. Pleskov, E.I. Terukov, O.I. Kon'kov, J. Electroanal. Chem. 600 (2007) 217.
[20] J.P. Maranchi, A.F. Hepp, P.N. Kumta, Electrochem. Solid-State Lett. 6 (2003) A198.
[21] J. Yin, M. Wada, K. Yamamoto, Y. Kitano, S. Tanase, T. Sakai, J. Electrochem. Soc. 153 (2006) A472.
[22] M. Saito, K. Nakai, M. Hagiwara, A. Tasaka, T. Takenaka, M. Hirota, A. Kamei, M. Inaba, ECS Trans. 25 (2010) 101.
[23] K. Nakai, I. Tsuchioka, M. Saito, A. Tasaka, T. Takenaka, M. Hirota, A. Kamei, M. Inaba, Electrochemistry 78 (2010) 438.
[24] B. Guo, J. Shu, Z. Wang, H. Yang, L. Shi, Y. Shi, Y. Liu, L. Chen, Electrochem. Commun. 10 (2008) 1876.